

Original Research Article

Evidence For Complex Physiological Processes In The Enamel Organ of The Rodent Mandibular Incisor Throughout Amelogenesis

Anas Falah Mahdee¹ Ahmed Ghanim Alhelal^{2*} John Whitworth¹
Jane Eastham¹ James Gillespie¹

¹Newcastle University, School of Dental Sciences, ENGLAND

² College of Dentistry, University of Babylon, IRAQ

*E-mail:ahmedghanim76@yahoo.com

Accepted 10 May, 2017

Abstract

The process of tooth formation and development is complex involving many signalling pathways and molecules. The enamel formation is a process controlled entirely by the enamel organ with many cell-cell interaction and signalling. Although this process was studied extensively, the full understanding is still to be achieved. Twenty dental pulps from rat mandibular incisor were dissected, fixed, frozen, sectioned, stained with specific antibodies then carefully examined using fluorescence microscope. The basic findings were cellular heterogeneity, presence of spherical vacuoles which may be blood vessels, and striking differential expression of some very important signalling molecules antigen throughout the enamel organ at different stages of development. This paper revealed some of the complexity associated with amelogenesis and proved that the previous description of enamel organ is very simplistic.

Key Words: enamel organ, amelogenesis, NaK-ATPase, NOS, Actin.

الخلاصة

ان عملية تكوين و تطوير الاسنان هي عملية معقدة تشمل على العديد من المسالك و الجزيئات التي تشارك في ارسال و استقبال الاشارات . عملية تكوين طبقة المينا تتم بالكامل عن طريق عضو تكوين المينا عن طريق العديد من التفاعل والاشارات بين الخلايا . على الرغم انه هذه العملية قد تمت دراستها على نطاق واسع ، لكن الفهم الكامل للعملية لم يتم الوصول اليه لحد الان . تم تجميع عشرون لب اسنان من السن القاطع السفلي للجرذان ، ثبتت ، جمدت ، تم تقطيعها ، صبغت بأجسام مضادة معينة ثم تم فحصها بعناية بأستعمال المجهر المتألق . الموجودات الاساسية من هذا البحث هي اكتشاف خلايا متنوعة و مختلفة ، اكتشاف فجوات كروية التي قد تكون اوعية دموية و بيان تواجد بعض الاجسام المضادة لجزيئات الاشارة في اماكن دون اخرى على طول طبقة المينا وعضو تكوين المينا و في مختلف المراحل التطورية . هذا البحث يكشف بعض التعقيد المتعلق بعملية تكوين المينا و اثبت ان الوصف السابق لعضو تكوين المينا مبسط جدا وغير وافي .

الكلمات المفتاحية : عضو تكوين المينا ، عملية تكوين المينا ، الصوديوم البوتاسيوم أيتيبيز ، انزيم تصنيع اوكسيد النتريك ، الاكتين .

Introduction

Ontogenesis is a highly-organised series of events started with the determination and localisation of the future teeth with distinct morphology and size. Advanced signalling cross-talks between mesenchymal cells and epithelium are necessary for the initiation and development of each tooth [1, 2].

Enamel organ is the part of the tooth germ that are responsible for the secretion and mineralising the enamel. It is composed of external and internal enamel epithelium, stellate reticulum and stratum intermedium. Enamel and organic matrix secretion and mineralisation is the product of a highly specialised cells called ameloblasts through a process called amelogenesis [3, 4].

It is well documented that the ameloblasts, in addition to the production and mineralisation of enamel, are also responsible for the elaboration of wide range of proteins into the organic matrix [5, 6]. Furthermore, ameloblasts are also considered as the major coordinator for the final rods and inter-rod architecture of enamel [7], such architecture are fundamental for enamel to withstand the masticatory forces [8].

Moreover, it is also hypothesised that ameloblasts rules the calcium and phosphate ions movement during amelogenesis [9, 10].

Amelogenesis can be divided into three main phases, secretory in which the enamel organic matrix is secreted with low mineral contents. The second phase shows enamel degradation and called transition phase, whereas large amounts of inorganic crystallites start to deposited and dominate the developing enamel in the third phase known as maturation phase [11-13].

The resulted enamel is brittle, hard and made mainly of inorganic hydroxyapatite crystals with minor fraction of organic matrix.

The current study utilized a contemporary immunohistochemistry to carefully examine the enamel organ of the rat

mandibular incisor to uncover some complexity.

Materials and Methods

Twenty lower incisors were carefully dissected from Wester male rats (300-400mg) that had been freshly killed by neck dislocation. The teeth were immediately fixed with 4% para-formaldehyde for 24 hours at 4°C, then demineralized in 17% EDTA with pH 7.4, for 4-6 weeks at 4°C with constant agitation [14]. After that the teeth were thoroughly washed with PBS for 10 minutes, before transfer to graded sucrose (10%, 20%, 30%) solutions for 24 hours in each at 4°C for cryoprotection. Samples were then placed in optimal cutting solution (OCT) (Sakura Finetck Europe B.V. Netherlands), snap frozen in isopentane and liquid nitrogen, and stored in -80°C. The frozen stored samples were subsequently mounted on a chuck piece in the cryostat chamber (Shandon, cryotome FSE, Thermo Fisher scientific, USA) at -25°C, sectioned longitudinally at 7µm and placed on polysine coated slides.

The Immunofluorescence staining procedure was performed as follows. The slides were washed with TBS, TBST, and TBS for 5 minutes each using a 3D rocking platform (Stewart Scientific, UK) before dividing them randomly into 3 staining groups (around 80 slides for each group) according to the type of primary antibody combination used. The first group was stained with monoclonal anti-vimentin structure protein (vim) (mouse 1:5000, Sigma) and monoclonal anti-NaK-ATPase enzyme (rabbit 1:500, Abcam), while the second group was also stained with anti-vimentin but also with polyclonal anti-neuronal nitric oxide synthase enzyme (eNOS) (rabbit, 1:500, Santa Cruz). The third group was stained with NOS and monoclonal anti-α smooth muscle actin (rabbit, 1:100, Abcam). The primary antibody combination was applied to each section before incubating slides in a humid atmosphere at 4°C for 24 hours. The following day, the slides

were washed in a three-stage cycle (TBS, TBST, and TBS) for 20 minutes each. The slides were then dried and placed in the humidifier at room temperature before applying the secondary antibody which was selected in accordance to the species of primary antibody that had been used. Donkey anti-mouse/rabbitIgG antibody conjugates, Alexa Fluor 488 (Molecular Probes®, Invitrogen) which target the first primary antibody were applied to the samples, incubated in the humidifier for one hour, then washed with (TBS, TBST, and TBS) for 20 minutes each. Subsequently, the second secondary antibody donkey anti-rabbitIgG antibody conjugates, Alexa Fluor 594 (Molecular Probes®, Invitrogen) which target the second primary antibody was applied before incubation in the humidifier for one hour. Finally, the slides were washed with (TBS, TBST, and TBS) for 20 minutes each before applying Vectashield hard set mounting medium with DAPI (nucleic acid molecular probe stain) (Vector Laboratories Inc, Burlingame) and glycerol with PBS and left for two minutes to set, then placing a glass cover slip, and sealing with a nail varnish around its margins.

Positive and negative control samples were used. In the positive controls the slides were incubated with PBS instead of the primary antibodies before staining with the secondary antibodies only. While in the negative controls the slides were incubated with PBS only as explained in [15].

The stained slides were examined at X10, X20, and X60 magnification with an Olympus BX61 microscope using Alexa Fluor 488 and 594 fluorochromes detected via the microscope light source and dichroic mirror to split excitation and emission light wavelengths. Relevant images were captured with a microscope-mounted Olympus XM10 monochrome camera and examined using Image J software (Java- based image processing program- National Institute of Health (USA)). Approximately 80 slides were

examined to confirm the accuracy and consistency of the staining technique and to reveal constant staining phenomena [16].

Results

The control samples did not exhibit any specific fluorescent labelling. The principle observations explored within this paper are illustrated in Figure 1. Panels A and B show the early and late secretory stages of enamel formation. Note that the boundary of the ameloblast and enamel is indentified by the dotted lines, as the ameloblasts, in this region, do not stain with NaK-ATPase. In contrast, immuno-reactivity to the NaK-ATPase (NaK-ATPase-IR) was located principally in the cells of the developing stratum intermedium (si) and stellate reticulum (sr). Panels C and D show the early and late maturation stages of enamel formation process respectively. NaK-ATPase-IR was found within all cells of the papillary layer. Immuno-reactivity to nitric oxide synthase (NOS-IR) was located more in cells of the stratum intermedium (si) in the secretory stages (E and F) but appeared in the early maturation phase, of enamel formation, in the ameloblasts and papillary layer. Note that NOS-IR is concentrated in the basal region of the ameloblasts in the late maturation stage.

Figure 2 illustrates the different cell layers within enamel organ in the secretory stage. In A, the section was stained with antibodies nitric oxide synthase (NOS, red), the structural protein vimentin (vim, green) and the nuclear stain dapi (blue). The different cell layers and structures are shown: ameloblast (am), stratum intermedium (si), stellate reticulum (sr), peridontium (pd) and enamel (en). The panels below illustrate the individual images that formed the colour composite. The cells of the stratum intermedium and stellate reticulum clearly showed NOS-IR with greater intensity of staining in the stratum intermedium cells (single image, arrows and see Figure 3). The ameloblasts,

particularly in their apical region, also showed NOS-IR. The nuclei of the ameloblasts were located in the basal region which may influence the apparent distribution of NOS-IR. However, in these cells the NOS-IR was less intense. Interstitial cells of the peridontium were vimentin immuno-reactive (vim-IR) and can be seen to lie also between the processes of the stellate reticulum cells. This is more easily seen in the single vimentin image (arrows). The enamel appears to stain with the vimentin antibody revealing the Tome's processes (tp) adjacent to the apical surface of the ameloblast. It is not known, at this stage, whether this staining is specific or non-specific. Figure 2 B illustrates the distribution of the enzyme NaK-ATPase. The lower panels show the separate images making the composite. The primary cells demonstrating NaK-ATPase-IR were in the stratum intermedium and stellate reticulum. Note the more intense staining in the stellate reticulum cells (arrows, see also Figure 4).

A more detailed illustration of the distribution of NOS-IR in the secretory stage is shown in Figure 3. Panel A shows an over view, with two regions of interest are identified as (a) and (b), focusing on the ameloblast and stratum intermedium respectively. In (a) dense NOS-IR is seen in the apical region of the ameloblast (arrows) and the relative position of this staining to the cell nucleus at the base of the cells is apparent. In (b) an intense NOS-IR in the stratum intermedium can be seen (see arrow in the individual NOS image). The vim-IR cells (green) of the peridontium are seen in the combined image (b) as are the NOS-IR cells of the stellate reticulum. Note that vim-IR cells appear to surround cell free spaces (vacuoles (v)) between the cell processes of the stellate reticulum (see also Figure 7).

Figure 4 shows details of the distribution of NaK-ATPase-IR in the secretory region. As described earlier, there is a highly-localised expression of NaK-

ATPase-IR within the cells of the stellate reticulum and stratum intermedium. The spaces between the stellate reticular processes that are surrounded by vim-IR cells can also be seen in panel B (*). Panel C, showing only NaK-ATPase-IR, demonstrates the weak immuno-reactivity in the stratum intermedium and stronger signal in the stellate reticulum.

Figure 5 compares the staining patterns for NaK-ATPase-IR and NOS-IR in the early and late stages of the maturation phase. A and B respectively show the early and late matured enamel organ expressed with NaK-ATPase-IR. Regions of interests are identified. In A (a1) the NaK-ATPase-IR in the ameloblasts is enhanced to illustrate its presence (arrows). In (a2) the loss of stratum intermedium and the more uniform NaK-ATPase-IR is illustrated in the papillary cells. In B, the late phase, NaK-ATPase-IR is seen in the ameloblasts and papillary layer but the papillary staining is less intense. In C and D the distribution of NOS-IR is shown for the early and late stages. There appears to be a reduction in NOS-IR in the apical region of the ameloblast in the late stage, but the intense staining in the basal region remains. In the papillary layer the NOS-IR remains uniform.

Actin-IR is not found in the ameloblasts or in the papillary layer. It is detected in the peridontial region (Figure 7). Panel A shows a low power overview demonstrating actin-IR in the spaces between the papillae and in a layer of cells immediately below the papillae. Panel B shows that the actin-IR appears to surround the spaces between the papillae giving the appearance of vacuoles. Actin-IR filaments can be seen to run between adjacent vacuoles (arrows). At higher magnification (C), there is a region immediately below the papillae which contains cells that are not actin-IR (black space). The nuclei of cells in this region can clearly be identified (*). Below this layer are cells that are actin-IR. Again, the nuclei of these cells, surrounded by actin-IR can be seen (▲).

The expression of NaK-ATPase-IR in the ameloblast cells during all stages of enamel formation is illustrated in Figure 8. In panel A, it appears that there is no NaK-ATPase-IR in ameloblast during secretory stage. Panel B shows the transitional zone where ameloblast cells change from no NaK-ATPase-IR (+) toward the apical direction (Ap) to more NaK-ATPase-IR in the basal region of

ameloblast cells (*) toward the incisal direction (Inc). Enhanced images of the early and late matured ameloblast layer are showed in panel C and D. Panels E and F illustrate the incisal end of the enamel organ where the ameloblasts and other cellular constituent this organ are reduced in size and number, with no NaK-ATPase-IR and seem to be similar to the adjacent periodontal cells.

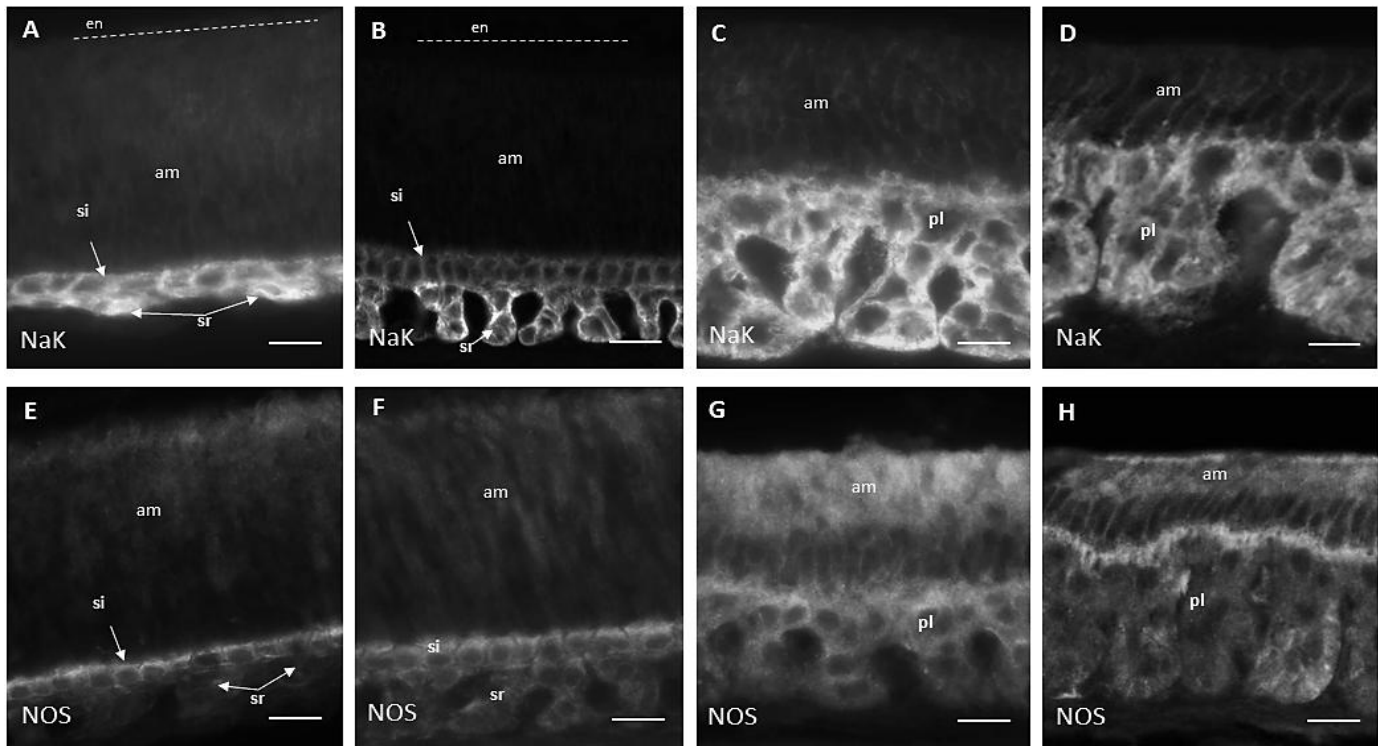


Figure 1: The regional expression of NaK-ATPase and NOS in the enamel organ at different stages of the enamel formation process. A illustrates the expression of NaK-ATPase in the outer enamel organ cells in the early secretory stage (the dotted lines show the boundary of the ameloblast which, in this region does not stain), B shows the secretory stage, C and D the early and late maturation stages respectively. E-H show the expression of NOS. E illustrates the expression of NaK-ATPase in the outer enamel organ cells in the early secretory stage, F the secretory stage, G and H the early and late maturation stages respectively. Note the difference in sizes of the stratum intermedium (si) and stellate reticulum (sr) between A and B (arrows) also between E (arrows) and F. Calibration bars: 15 μ m in A, B, E and F, 10 μ m in C and D and 15 μ m G and H.

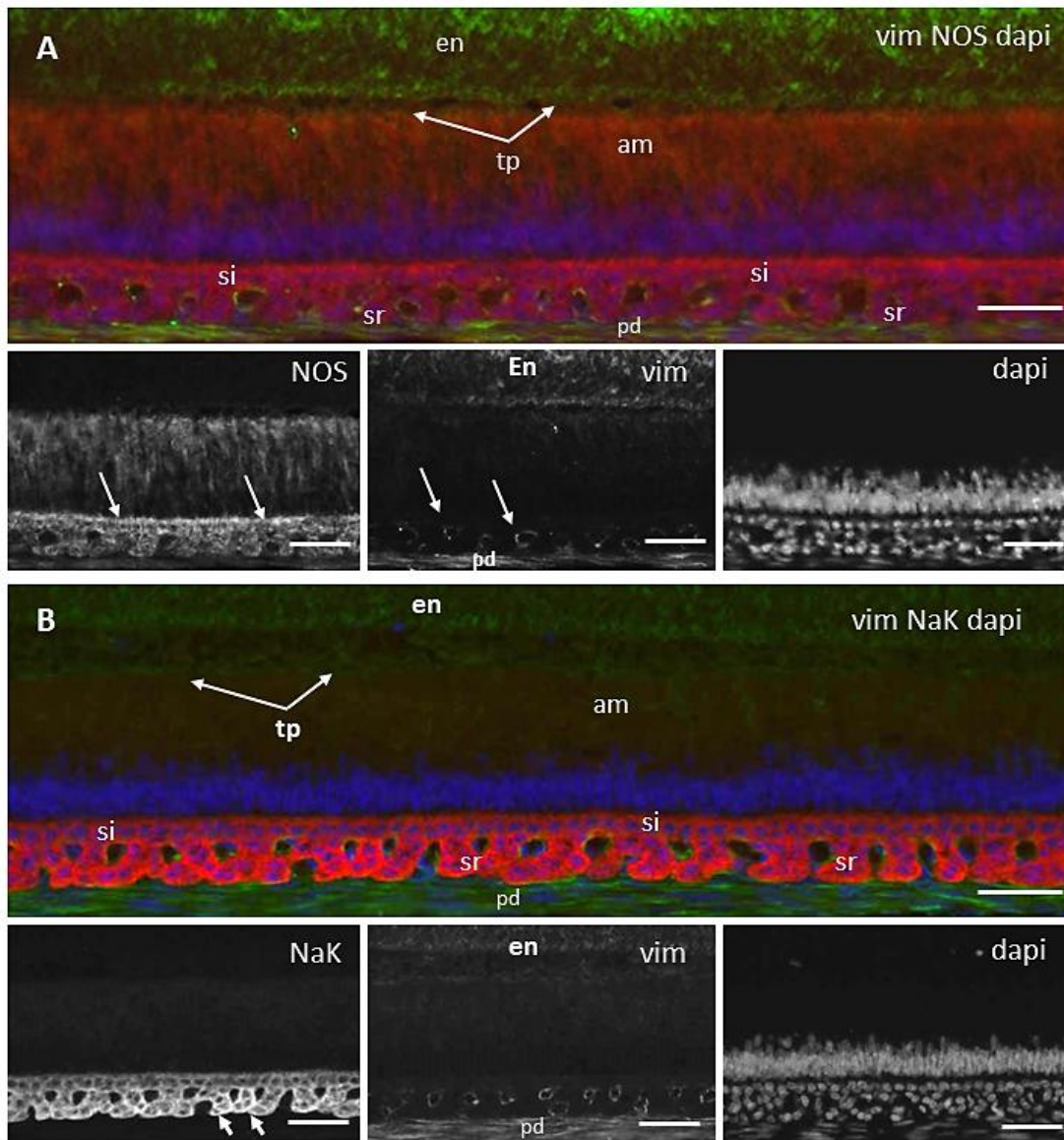


Figure 2: Images comparing the expression of nitric oxide(NOS)and NaK-ATPase synthase in the secretory stage of enamel formation. Section A was stained with vimentin (green), NOS(red), and dapi (blue) and B withNaK-ATPase (red), vimentin (green), and dapi (blue).The following structures were identified: en; enamel, am; ameloblast cell layer, si; stratum intermedium cell layer, sr; stellate reticulum cells, pd; periodontium connective tissue.In A the ameloblasts (am) were positive for NOS as were the stratum intermedium and stellate reticulum cells. The lower three panels show the component images for NOS, vimentin and dapi. In B, no expression of NaK-ATPase was seen in the ameloblast (am) or peridontium (pd). However, the stratum intermedium and stellate reticular cells were strongly NaK-ATPase positive. The lower three panels show the component images for NaK-ATPase, vimentin and dapi. Calibration bars: 60 μ m in the composite images A and B.

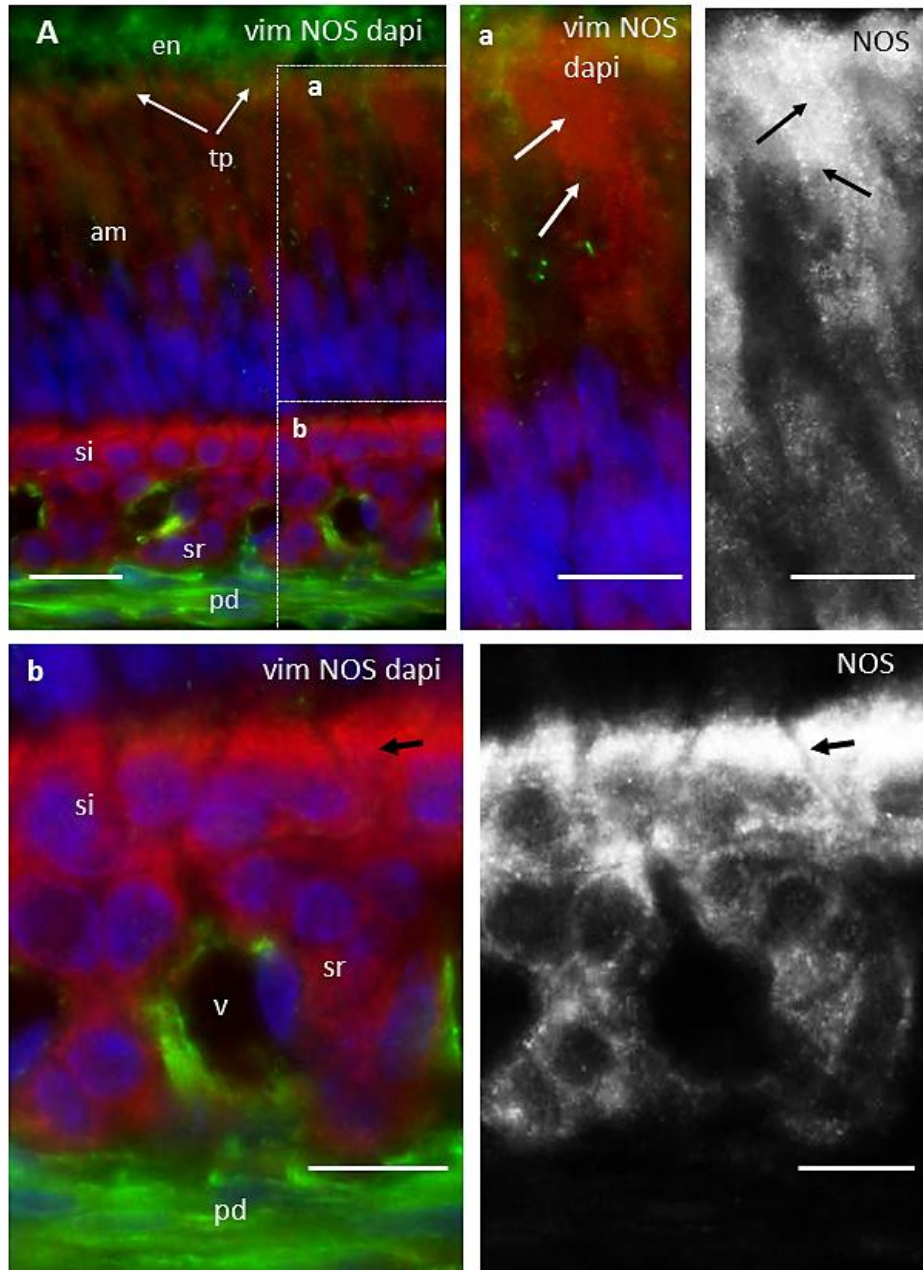


Figure 3: Higher magnification images illustrating the distribution of NOS in the secretory stage. A shows a section of the entire cellular structure of enamel organ stained for NOS (red), vimentin (green), and dapi (blue). The boxes marked by the dotted lines (a) and (b) show sections of the organ illustrating the ameloblast (am) and stratum intermedium (si) respectively. In (a) the black and white images show the localisation of NOS within the ameloblast. Note the more intense staining in the apical region (arrows). (b) shows NOS staining in the stratum intermedium, which appeared to be more than stellate reticulum cells (sr). Also in (b) vimentin positive interstitial cells of the periodontium were seen to surround non-cellular spaces (vacuoles (v)) (see also Figure 1). Calibration bars: upper left panel 30 μ m, (a) 20 μ m and (b) 15 μ m.

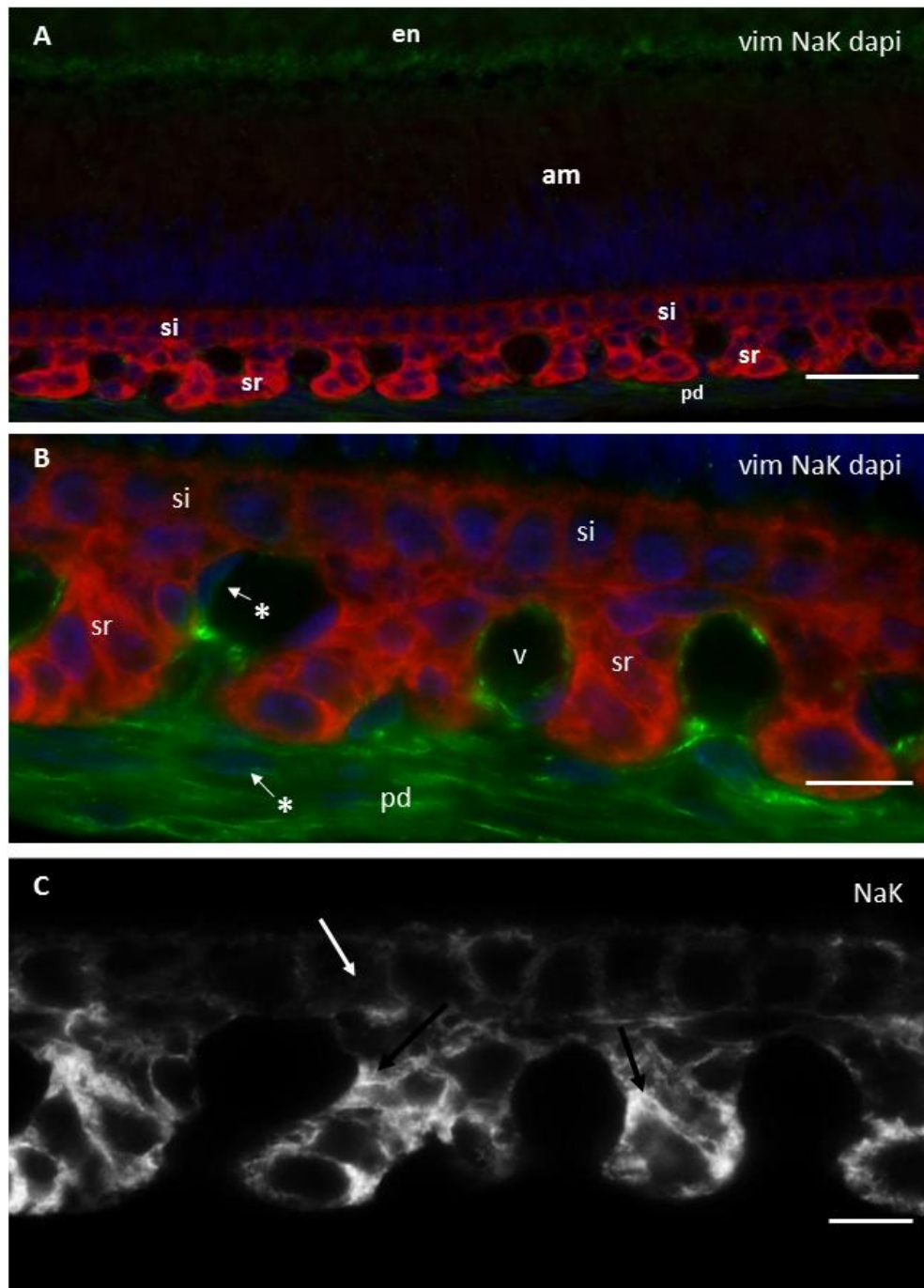


Figure 4 :Cellular and non-cellular layers in the secretory stage of enamel formation. A shows a low power image of a section stained with antibodies to vimentin (green), NaK-ATPase (red), and dapi (blue).B is magnified region from panel A showing stratum intermedium, stellate reticulum and periodontal connective tissue. Note, the presence of large vacuoles beneath the stellate reticulum surrounded by nucleated vim⁺ periodontal interstitial cells (*). Cshows the original single wavelength image illustrating the distribution of NaK-ATPase. Note, the higher intensity of staining in the stellate reticular cells (white arrow) compared to the stratum intermedium (black arrows). Calibration bars: 50 μ m in A and 15 μ m in B and C.

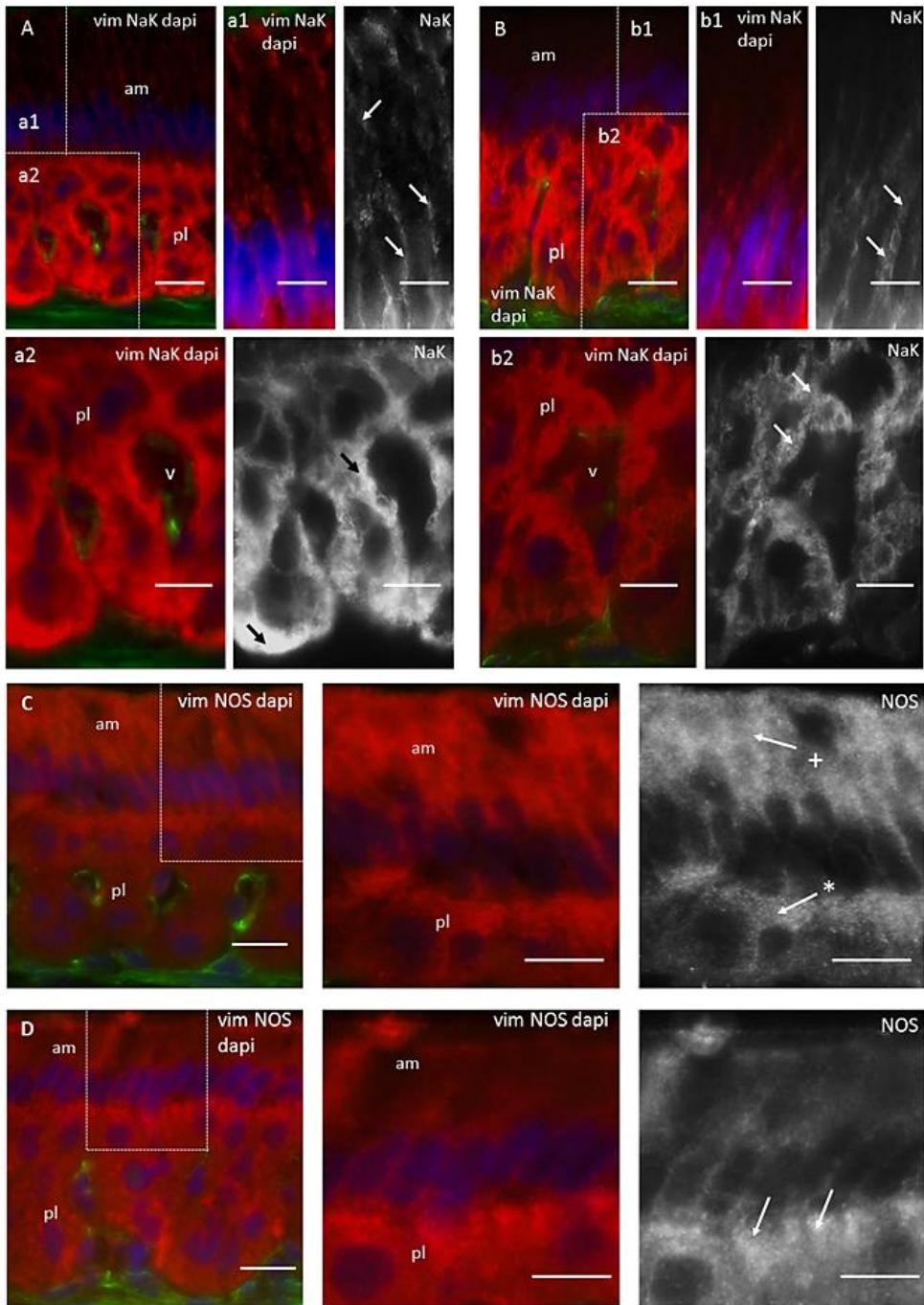


Figure 5: Higher resolution images showing the distribution of NaK-ATPase and NOS in the early and late maturation stages. A and B show staining for NaK-ATPase (red), vimentin (green), and dapi (blue) to show nuclei. In A positive staining was observed in both ameloblast and papillary layers. The boxes, identified a1 and a2, represent specific regions of interest. Weak staining was observed in the ameloblasts (see enhanced images in (a1)). Note that the NaK-ATPase staining appears to be located on the surface of the ameloblasts (arrows). In contrast, intense staining was observed in all cells of the papillary layer (a2). B shows NaK-ATPase distribution in the late maturation phase. Again the intensity of NaK-ATPase staining was lower in the ameloblast compared to the papillary layer. Note the possibility that the expression of NaK-ATPase was reduced in the papillary layer in the late maturation phase. C and D show staining for NOS (red) vimentin (green) and dapi (blue) in the early and late maturation stages respectively. In C a higher intensity of staining for NOS is seen in the ameloblast compared to the papillary layer. Also, note higher NOS staining in the basal region of the ameloblast (*) compared to the apical region (+). In

D, the late maturation phase, note the relatively higher NOS staining in the basal region of the ameloblast. Calibration bars: 60 μ m in A and B.

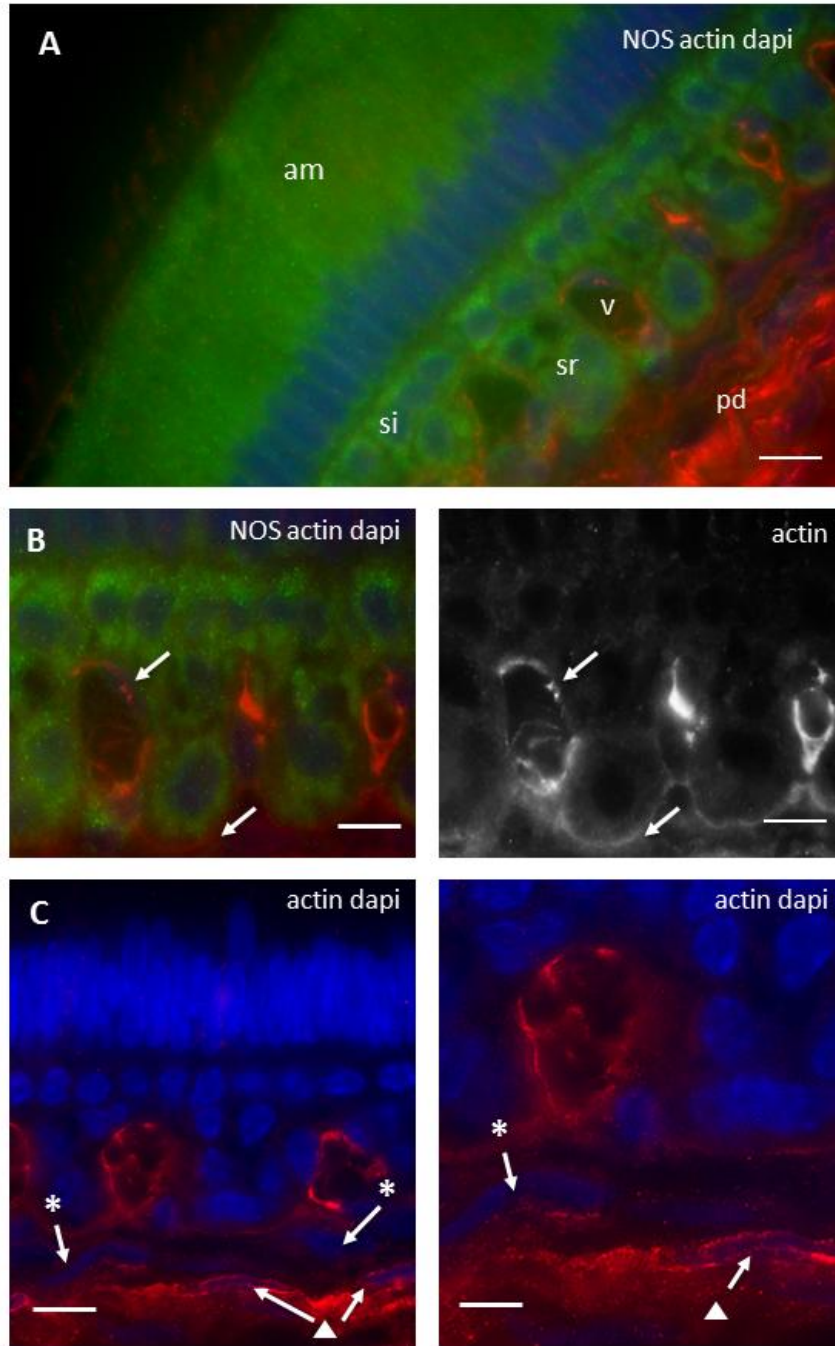


Figure 6: The distribution of actin filaments in the secretory stage of enamel formation. A shows a low power image of a sections stained for NOS (green), actin (red) and dapi (blue). Note the presence of actin filaments in the interstitial cells in regions of the peridontium (pd) and surrounding the spaces between the papillae (v). B shows, at higher magnification, actin fibres within the cells that form vacuoles (arrow) between the papillary cells. These are the vimentin⁺ cells described in Figure 3. C shows details of the peridontial region. Note (i) cells containing actin filaments surrounding the vacuoles, (ii) cells immediately below the papillary layer that are not actin-IR (note the nuclei of these cells (*)) and (iii) cells below the layer (ii) that are actin-IR (the nuclei of these cells is shown (▲)). Note also the complex actin-IR within one of the vacuoles in this section. Calibration bars: A, 25 μ m and 15 μ m in B and C.

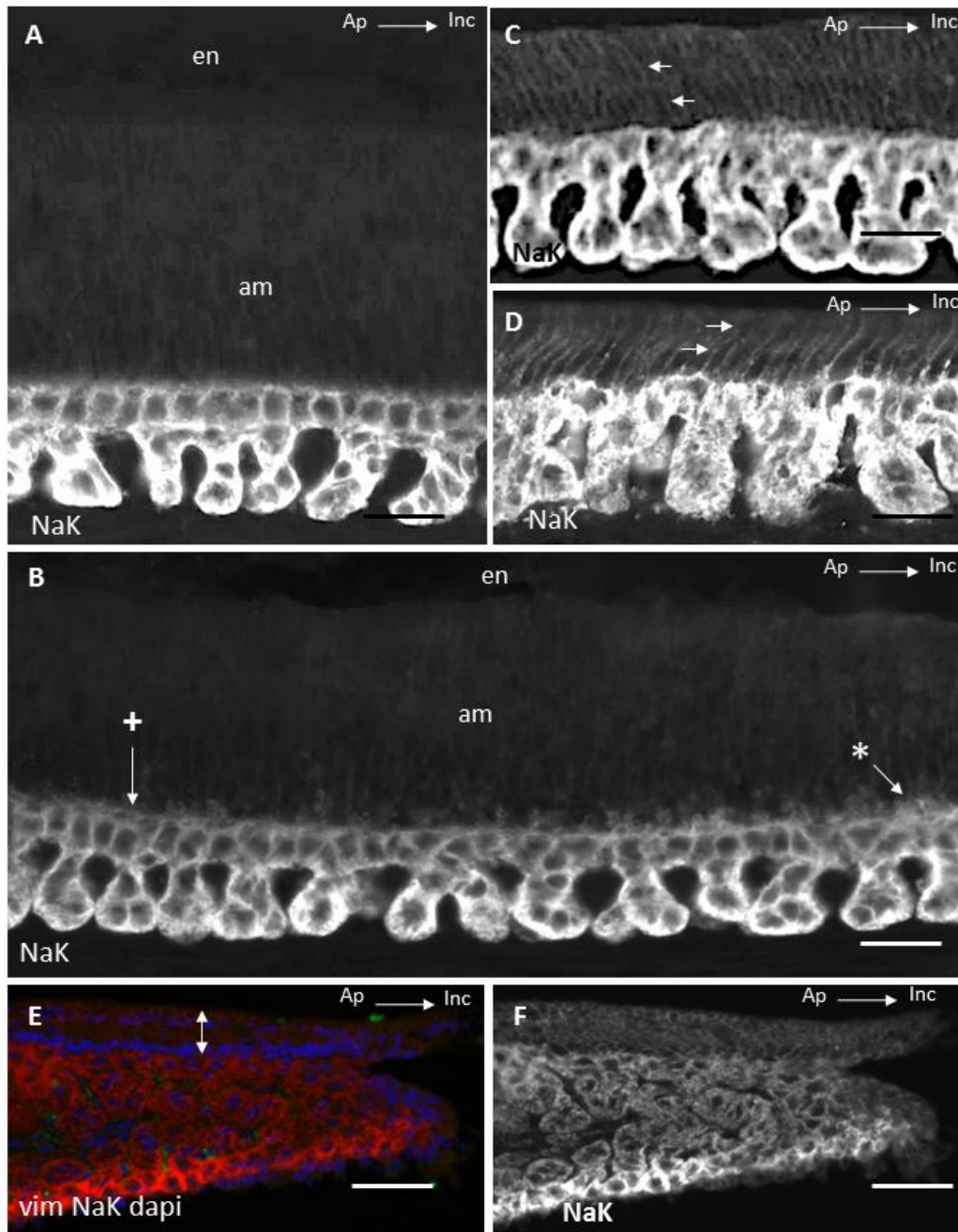


Figure 7: The expression of NaK-ATPase in ameloblasts in different stages during the process of enamel formation. A illustrates the secretory ameloblast. Note the absence of any significant NaK-ATPase in the ameloblasts. B shows a section illustrating the transitional zone. Ameloblasts (am) towards the apical direction do not express NaK-ATPase (+) while ameloblasts towards the incisal direction express NaK-ATPase (*) in the basal region of the cells. C and D show respectively the early and late maturation stages. Note that the ameloblasts now express NaK-ATPase and that the orientation of the cells changes: in the early stage the cells slope towards the apical side, while toward the incisal direction in the late stage. E and F shows incisal end of the enamel organ. Calibration bars: 20 μ m in A-D and 60 μ m in F.

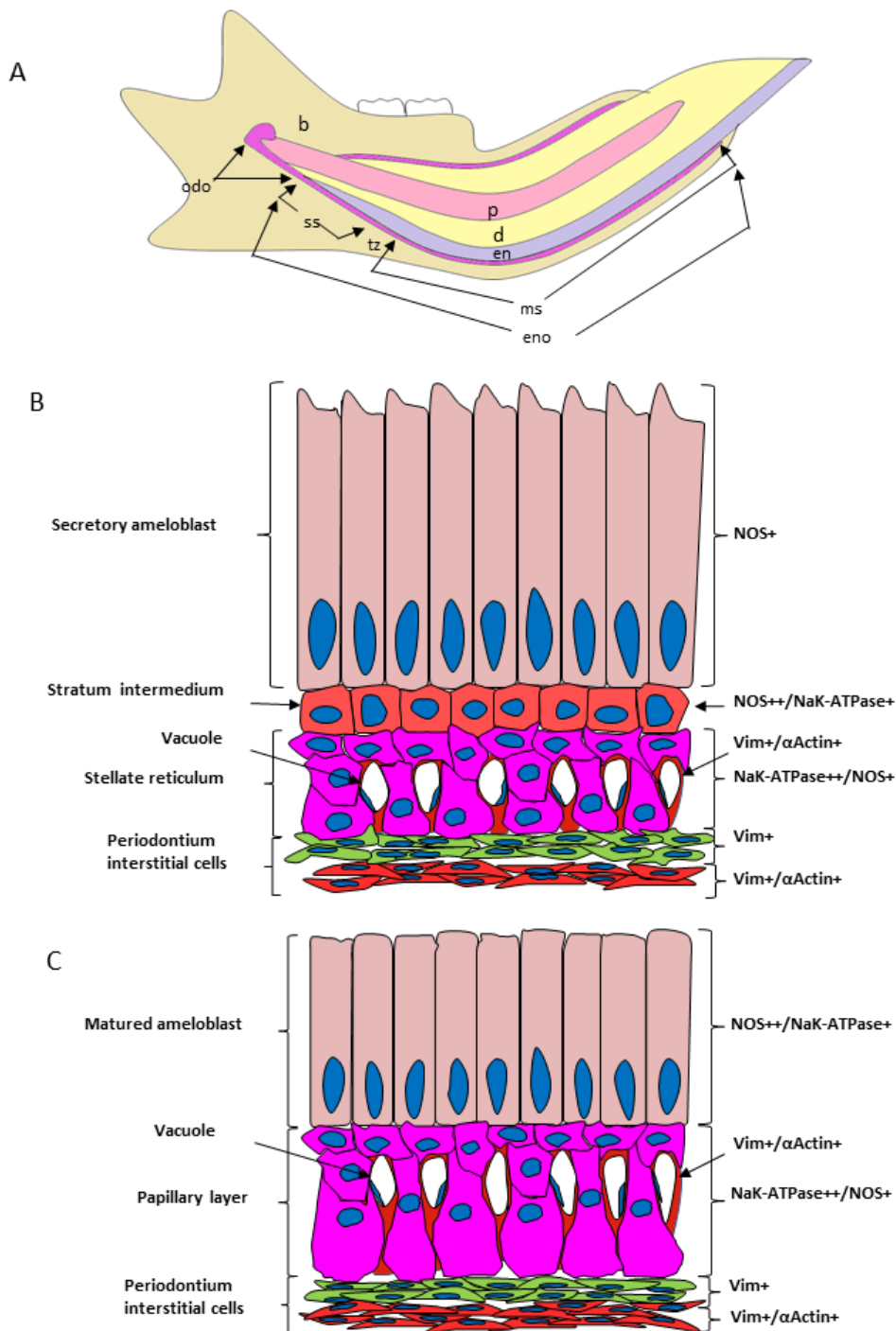


Figure 8: Cartoon illustrating the different regions of the rodent incisor (A) and (B) and (C) a summary of the observations on the structural components of secretory and maturation parts of the enamel organ. In A the following regions are identified: *b*, mandible bone; *odo*, odontogenic organ; *p*, pulp; *d*, dentine; *en*, enamel; *eno*, enamel organ. The different regions of the enamel organ are identified: *ss*, secretory stage; *tz*, transitional zone; *ms*, maturation stage. B, the different cell layers of the enamel organ are identified. The expression and the levels of expression for the antibodies used in this study (NOS, vimentin, NaK-ATPase, and actin) are also shown. A similar description of the cell layers in the maturation stage is shown in C and the location and levels of the same panel of antibodies.

Discussion

In the current study, the dental pulp from rat mandibular incisor has been used as an experimental model for many reasons. First it is readily available, well established in the literature and share many similarities and differences with human dental pulp. One of the most excellent features of the rat incisor dental pulp is the continuous growth which provide an excellent model to observe the tooth development and all stages at the same time and in one sample [17].

The immunohistochemical technique utilized in this study is essential to observe the various cellular and tissue antigens. [18] hypothesized that cell markers immunohistochemistry provide a method to talk with cells, because it grants a way of identification of the histological architecture of the cells as well as indicating the function if the suitable antibodies used.

It is not logical and unsatisfactory to consider the immunohistochemistry as a descriptive method only, in fact the invitro and in situ experiments can be regarded as accurate pictures to in vivo situations [18].

It is becoming progressively accepted that the histological and functional description of the enamel organ explained in the introduction is too simplistic, for example, ameloblasts have been found to secrete various proteins not only during the secretory phase but throughout their life in variable magnitudes. The cellular component of enamel organ is controlled by many signalling molecules like components of extracellular matrix and growth factors to guide the process of secretion and maturation of enamel.

NaK ATPase is an enzyme responsible for pumping the Na ions to the extracellular space and moving the K ions intracellularly against their concentration gradient in an active process (consumes energy). This active transport help to preserve the cell resting action potential and monitor the cell size [19]. NaK ATPase may also function as a signalling molecule in many physiological

pathways, neurons and play a role in regulating the intracellular calcium [20]. It has been found that NaK-ATPase-IR is widely distributed in the dental pulp including many cellular systems [21] and found to play a crucial role in regulating the transmembrane ionic transport and balance.

Observation from the current study showed that NaK-IR was found primarily in the sub-ameloblast area at the secretory stage with completely negative IR in the ameloblasts area. In the maturation stage, the ameloblasts start to show NaK-IR but this expression was lost again at the end of amelogenesis where the enamel organ is nearly functionless. This variable expression may reflect the activity of different components of enamel organ at each stage as NaK ATPase can be regarded as marker for cell activity. It may also provide a picture about which cell layer consumes more energy and works more and the late participation of ameloblasts. It is apparent that the ameloblast cells expressed NaK-ATPase-IR (as seen in figure 5), but the more interesting observation that these cells change their orientation from apical to incisal during early and late maturation stages respectively.

Nitric oxide produced by nNOS (NOS1 used in the current study) can be regarded as a neurotransmitter and signalling molecule which helps in reducing the smooth muscles and blood vessels tone [22] and has a role in memory, learning and neurogenesis [23].

Ameloblasts, throughout the enamel-ogenesis, have been found to express NOS-IR which provide a clue that ameloblasts may have a signalling function or play a role in controlling the vascular tone. The sustainability of this positive IR reflects that the related function is continuous throughout amelogenesis.

The coupled and continuous positive expression of NaK ATPase and NOS in the papillary layer provide an evidence about the crucial contribution of these layers at all stages of amelogenesis.

One of the new findings in the current study is the observation of a large vacuoles beneath the stellate reticulum surrounded by nucleated vim+ periodontal interstitial cells. In all sections from all preparations these structures were mainly spherical or ovoid. No tubules were seen, suggesting that these structures are primarily spherical. The precise nature and function of these circular structures, is unclear.

Additionally, cellular heterogeneity was observed, where some cells show actin-IR. Re-examination of Figures 3 and 4 shows clearly that both cell types in this region, those that are actin-IR and those that are not, are all vim-IR. Thus, there are two populations of interstitial cells in the periodontal space.

Collectively, these observations demonstrate the expression of different functional elements and processes in the different cell layers of the enamel organ. This must imply that such specialisations underlie specific functional properties in the different cell layers.

References

1. Mina, M. and E. Kollar, The induction of odontogenesis in non-dental mesenchyme combined with early murine mandibular arch epithelium. *Arch Oral Biol*, 1987; **32**(2): 123-127.
2. Thesleff I, et al., Epithelial-Mesenchymal Signaling during Tooth Development. *Connective tissue Res*, 1995; **32**(1-4): 9-15.
3. Beeman CS, JE. Kronmiller. Temporal distribution of endogenous retinoids in the embryonic mouse mandible. *Arch oral biol*, 1994; **39**(9): 733-739.
4. Miller, N., Ten Cate's oral histology. *Bri Dent J*, 2012. **213** (4): 194-194.
5. Deutsch, D., Structure and function of enamel gene products. *The Anatomical Record*, 1989; **224** (2): 189-210.
6. Nanci A, CE. Smith. Development and calcification of enamel. *Calcification in biological systems*. CRC Press, Boca Raton, 1992; 313-343.
7. Warshawsky H, et al. The development of enamel structure in rat incisors as compared to the teeth of monkey and man. *The Anatomical Record*, 1981; **200**(4): 371-399.
8. Smith, C., Cellular and chemical events during enamel maturation. *Critical Rev Oral Biol Med*, 1998; **9**(2): 128-161.
9. Bawden, J.W., Calcium transport during mineralization. *The Anatomical Record*, 1989; **224**(2): 226-233.
10. Takano, Y., M. Crenshaw, and J. Bawden, Calcium movement in vivo and in vitro in secretory-stage enamel of rat incisors. *Arch oral biol*, 1992; **37**(5): 377-383.
11. Paine, M.L., et al., Regulated gene expression dictates enamel structure and tooth function. *Matrix Biol*, 2001; **20**(5): 273-292.
12. Robinson, C., et al., Matrix and mineral changes in developing enamel. *J Dental Res*, 1979; **58**(2_suppl): 871-882.
13. Bronckers, A., et al., Degradation of hamster amelogenins during secretory stage enamel formation in organ culture. *Matrix biology*, 1995. **14**(7): p. 533-541.
14. Cho, A., et al., A method for rapid demineralization of teeth and bones. *The open Dent J*, 2010; **4**:223-229.
15. Mahdee A, et al., Complex cellular responses to tooth wear in rodent molar. *Arch Oral Biol*, 2016; **61**: 106-114.
16. Gillespie JI, et al., Interstitial cells and cholinergic signalling in the outer muscle layers of the guinea-pig bladder. *BJU Int*, 2006; **97**(2): 379-385.
17. Ohshima, H. and S. Yoshida, The relationship between odontoblasts and pulp capillaries in the process of enamel-and cementum-related dentin formation in rat incisors. *Cell and tissue Res*, 1992; **268**(1):51-63.
18. Brandtzaeg, P., The increasing power of immunohistochemistry and immunocyto-chemistry. *J immunol meth*, 1998; **216** (1): p. 49-67.
19. Hall, J.E., Guyton and Hall textbook of medical physiology. 2015: Elsevier Health Sciences.
20. Howarth C, P. Gleeson, D. Attwell. Updated energy budgets for neural computation in the neocortex and cerebellum. *J Cerebral Blood Flow Metabol*, 2012; **32**(7): 1222-1232.

21. Duan, X., Ion Channels, Channelopathies, and Tooth Formation. *J Dent Res*, 2014; **93**(2): p. 117-125.
22. Förstermann, U. and W.C. Sessa, Nitric oxide synthases: regulation and function. *European heart J*, 2012; **33**(7): p. 829-837.
23. Zhou, L. and D.-Y. Zhu, Neuronal nitric oxide synthase: structure, subcellular localization, regulation, and clinical implications. *Nitric Oxide*, 2009; **20**(4): 223-230.